Distribution of Pigment Particles in Aqueous Drainage Structures in a DBA/2J Mouse Model of Pigmentary Glaucoma

Liping Pu, Rongyao Zhou, Qian Li, and Guoping Qing

Beijing Tongren Eye Center, Beijing Tongren Hospital, Capital Medical University, Beijing Ophthalmology and Visual Sciences Key Laboratory, Beijing, China

Correspondence: Guoping Qing, Beijing Tongren Eye Center, Beijing Tongren Hospital, Capital Medical University, Beijing Ophthalmology and Visual Sciences Key Laboratory, No. 1 Dongjiaominxiang Street, Dongcheng District, Beijing 100730, China;
gptsing@mail.ccmu.edu.cn.

Received: December 11, 2021
Accepted: May 15, 2022
Published: June 1, 2022

Citation: Pu L, Zhou R, Li Q, Qing G. Distribution of pigment particles in aqueous drainage structures in a DBA/2J mouse model of pigmentary glaucoma. *Invest Ophthalmol Vis Sci.* 2022;63(6):2.
https://doi.org/10.1167/iovs.63.6.2

Purpose. To characterize the distribution of pigment particles in aqueous drainage structures of DBA/2J mice with different intraocular pressure (IOP) levels.

Methods. DBA/2J mice were monitored from 9 to 44 weeks of age. IOP measurements were performed periodically. At 12, 20, 28, and 36 weeks, three mice were randomly selected for each time point and divided into three IOP groups. The morphology, size, and quantity of pigment particles in aqueous drainage structures were determined via transmission electron microscopy combined with ImageJ-based analysis. Between-group differences were evaluated with a one-way analysis of variance and Fisher's least significant difference test.

Results. In the anterior chamber, 74.2% (187/252) of pigment particles were round (diameter range, 0.20–0.73 µm), and 25.8% (65/252) were oval (length range, 0.35–1.20 µm). In the high-IOP group (IOP≥15 mmHg), pigment particles in the trabecular meshwork (TM) were more abundant and larger in size than those in the normal-IOP group ($P<0.001$). All separate pigment particles in the TM of the high-IOP group were >0.4 µm in size. The diameters of round (IOP≤10 mmHg, 0.44±0.13 µm; IOP between 10 and 15 mmHg, 0.57±0.13 µm; IOP≥15 mmHg, 0.61±0.12 µm) and the lengths of oval (0.65±0.14 µm vs. 0.77±0.12 µm vs. 0.88±0.15 µm, respectively) pigment particles in the TM differed among groups ($F=27.258$ and $F=27.295$, respectively; both $P<0.001$). No such differences were discovered in the iris and around Schlemm's canal ($P>0.05$).

Conclusions. In DBA/2J mice, large and medium pigment particles (>0.4 µm) seem to play an important role in causing aqueous outflow obstruction and IOP elevation.

Keywords: DBA/2J mice, pigment particles, pigmentary glaucoma, aqueous drainage structure, intraocular pressure

Pigmentary glaucoma (PG) is a form of secondary open-angle glaucoma with a relatively simple pathogenesis. In contrast to other types of glaucoma, PG is characterized by the accumulation of pigment particles within the trabecular meshwork (TM), resulting in intraocular pressure (IOP) elevation and glaucoma.[1,2] These pigment particles not only cause mechanical obstruction of the intertrabecular spaces but also lead to loss of trabecular cells that phagocytize pigment particles, fusion of trabecular lamellae, and collapse of the intertrabecular spaces, as well as obliteration of the canal.[3,4] However, the mechanisms by which pigment particles trigger the obstruction of the TM are still not fully clear.

The wide use of DBA/2J mice, a classical animal model of PG, has provided new insights into these complex processes.[5–7] DBA/2J mice develop an age-related form of glaucoma that replicates the clinical features of PG, including progressive iris pigment dispersion, iris stromal atrophy, iris transillumination defects, ocular hypertension, and retinal ganglion cell degeneration.[8] However, the development of glaucoma in DBA/2J mice is spontaneous, chronic, and variable, presenting a big challenge for researchers. Previous studies have demonstrated that specific mutations in the *Gpnmb* (*Gpnmb*^{R150X}) and *Tyrp1* (the *Tyrp1*^{b} allele) genes, which encode melanosomal proteins, induce PG in DBA/2J mice.[5] Additionally, Scholz et al.[9] noted that a narrowed anterior chamber (AC) angle may aggravate aqueous outflow obstruction. On the other hand, Schraermeyer et al.[10] reported that an insubstantial number of extracellular pigment particles were observed in the TM of DBA/2J mice. The aqueous drainage channels were blocked by pigment-laden macrophages instead of by cell debris or melanosomes. Nonetheless, the accumulation of pigment particles in the TM is a risk factor for the progression of glaucoma, and all current treatments aim to reduce their production.

As an important component of the aqueous drainage structures, the TM is composed of microtubular structures that form connections, with gaps of varying sizes in between.[11,12] The diameters and contractility of these microtubules and gaps determine their maximum passing capacity. Based on our preliminary research, we speculated that there is a maximum permeable diameter (MPD) for pigment

Copyright 2022 The Authors

This work is licensed under a Creative Commons Attribution-NonCommercial-NoDerivatives 4.0 International License.

Investigative Ophthalmology & Visual Science

particles to pass all the way through the TM via the aqueous convection current. Pigment particles with diameters > MPD would not be able to flow into the downstream of the aqueous drainage channels and would be restricted to the intertrabecular spaces or the collecting tube, resulting in aqueous drainage obstruction and IOP elevation. At the same time, pigment particles with diameters≤MPD would be able to pass through the microtubules and gaps and finally migrate out of the eye.

The aim of this study was to investigate the relationship between the distribution of pigment particles and IOP in a DBA/2J mouse model of PG. We also aimed to test the above hypothesis by comparing the morphology, size, and quantity of pigment particles in aqueous drainage structures of DBA/2J mice with different IOP levels by using transmission electron microscopy combined with analysis based on ImageJ (National Institutes of Health, Bethesda, MD, USA).

Materials and Methods

Animals and Husbandry

The experimental protocol was approved by the Animal Experimentation and Laboratory Animal Welfare Committee of Capital Medical University (project number AEEI-2020-194). All procedures were conducted in accordance with the ARVO Statement for the Use of Animals in Ophthalmic and Vision Research. DBA/2J mice (Beijing HFK Bioscience Co., Ltd., Beijing, China) were housed under specific pathogen-free conditions at the Laboratory Animal Department of Capital Medical University. All mice were kept at a room temperature of 21° ± 2°C with a 12-hour light–dark cycle and fed ad libitum.

Twenty male DBA/2J mice, from 9 to 44 weeks of age, were examined at regular intervals. Mice 12, 20, 28, and 36 weeks old were randomly selected (three mice for each time point) and divided into three IOP groups (≤10 mmHg, 11 eyes; between 10 and 15 mmHg, six eyes; ≥15 mmHg, seven eyes), based on their IOP measurements before they were sacrificed. An IOP≥15 mmHg was considered elevated.[13]

IOP Measurements

Mice were weighed and kept in a rodent-specific anesthetic machine (R510-31; RWD Life Science Co., Ltd., Shenzhen, China), and the percentage of isoflurane (RWD Life Science Co., Ltd.) in the evaporation tank was set to 3%. Initially, mice were sedated with 5 L/min of isoflurane for 1 minute. The sedated mice received 0.8 to 1 L/min of isoflurane for 4 minutes to maintain the anesthesia.[14] We measured the IOP sequentially six times (three for the right eye and three for the left eye) for each mouse by using an iCare TONOLAB Tonometer (iCare Finland Oy, Vantaa, Finland).[15] The average of three repeated measurements was used as the final IOP value. All data were collected by the same operator between 10:00 AM and 12:00 PM.

Anterior Segment Morphology

Morphological changes in the anterior segments of DBA/2J mice were monitored with slit-lamp microscopy at 25× or 40× magnification at 12, 20, 28, 36, and 44 weeks of age. All photographs were taken under identical settings.

Extraction and Measurement of Pigment Particles in the Anterior Chamber

Pigment particles were extracted from the AC of DBA/2J mice 36 weeks of age (as the iris depigmentation was most prominent in these), according to a protocol used in two previous studies.[16,17] Briefly, eyes were purified in 5% povidone iodine (Alcon, Fort Worth, TX, USA) for 2 minutes, and the lenses, ciliary bodies, and posterior segments were removed. The anterior segments were stored in phosphate-buffered saline (PBS), frozen at −80°C for 2 hours, and thawed at room temperature. Thereafter, the tissue samples were pipetted up and down 100 times, and cell debris was filtered through a 40-µm cell strainer (Corning Inc., Corning, NY, USA). After centrifugation for 15 minutes at 3000 rpm, the supernatant was discarded. This was repeated once, and the precipitate was resuspended in 2 mL of PBS and stored at 4°C.

Then, 10 µL of the suspension was added to carbon-coated copper grids, allowed to stand for 10 minutes, and air-dried at room temperature. The pigment particles were examined by using a transmission electron microscope (HT7700; Hitachi High-Technologies Corp., Tokyo, Japan). ImageJ 1.80 was applied to measure the diameters of 100 randomly selected pigment particles. This process was repeated three times by the same operator, and the average diameter of the 100 particles was calculated.

Light and Electron Microscopy

The eyes were fixed in 4% paraformaldehyde (Solarbio Science & Technology Co., Ltd., Beijing, China) for 48 hours at 4°C. After dehydration in a graded series of ethanol solutions (70%, 80%, 90%, 95%, and 100%), samples were transferred to xylene and embedded in paraffin wax (Solarbio Science & Technology Co., Ltd.). Subsequently, 4-µm-thick sections were prepared with a paraffin slicer along the sagittal axis of each eye (RM2235; Leica Microsystems GmbH, Wetzlar, Germany), stained with hematoxylin and eosin (H&E), and examined with a light microscope (DM4000; Leica Microsystems GmbH). The focus was on aqueous drainage structures and the distribution of pigment particles.

The eyes were fixed in 2.5% glutaraldehyde (Solarbio Science & Technology Co., Ltd.) for 2 hours at 4°C. Thereafter, tissue from the AC angle was divided into 2-mm × 2-mm pieces and fixed under the same conditions for an additional 12 hours. After being washed with phosphate buffer, samples were added to 1% osmium; dehydrated in a graded series of 50%, 70%, 80%, and 90% ethanol; transferred first to 100% ethanol and second to 100% acetone; and embedded in EPON 812 (SERVA Electrophoresis GmbH, Heidelberg, Germany). Ultrathin sections (50–70 nm) were prepared, stained with uranyl acetate and lead citrate, and examined under a transmission electron microscope. The morphology, size, and quantity of pigment particles were observed in the aqueous drainage structures, 100 of which were randomly selected for measurement of their diameters. The measurement method was the same as stated in the previous subsection.

Statistical Analysis

In this study, the minimum sample size was determined using G*Power 3.1.9.7 Software (Heinrich-Heine-Universität

Investigative Ophthalmology & Visual Science

Düsseldorf, Düsseldorf, Germany), based on the results of our unpublished pilot study. The calculation indicated that at least 15 subjects (n=5 per group) were required to achieve a power of 0.80, an effect size of 0.92, and an alpha of 0.05. All data in this report were derived from samples that exceeded the above required sizes.

All data analyses were performed by using SPSS Statistics 25.0 for Windows (IBM Corp., Armonk, NY, USA) and Prism 8.0 (GraphPad Software, Inc., San Diego, CA, USA). Quantitative variables were described as the mean±standard deviation. The differences in pigment particle size in the aqueous drainage structures of DBA/2J mice among different IOP groups were evaluated by using a one-way analysis of variance, followed by Fisher's least significant difference test. Differences were considered statistically significant at P<0.05.

Results

IOP Fluctuations

Twenty DBA/2J mice (40 eyes) were used; however, three mice did not survive to 20 weeks, and one eye was affected by spontaneous hyphema at 44 weeks. Seventeen mice (33 eyes) were included in the analysis. Eyes that developed corneal abnormalities were not excluded. The IOPs of the DBA/2J mice started to increase from 24 weeks onward. At the age of 28 weeks, 13 of 21 eyes (62%) developed IOP>10 mmHg. Up to 36 weeks, 10 of 15 eyes (67%) exhibited an IOP≥15 mmHg. As shown in Figure 1, the average IOP of the mice increased with age, peaked at 36 weeks, and subsequently decreased. At the age of 44 weeks, more than half of the mice had an IOP within the normal limits. Group allocation was only performed for mice up to 36 weeks old.

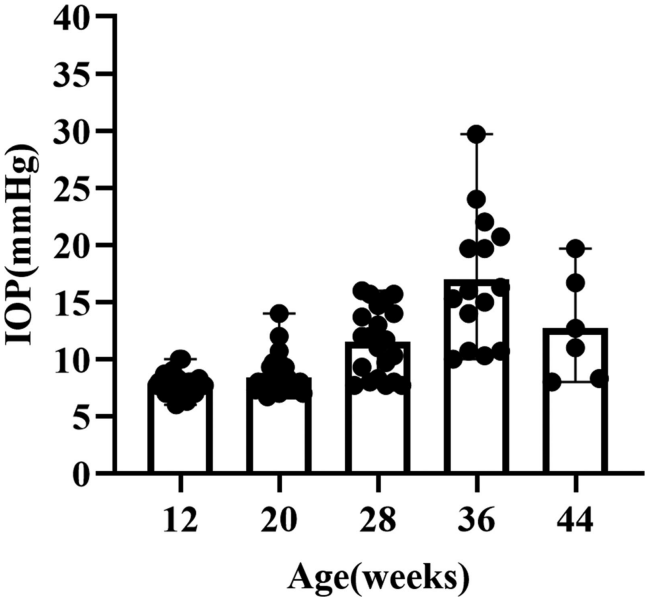

Figure 1. Changes in IOP (means±ranges) in DBA/2J mice of different ages (n=33, 27, 21, 15, and 6 at 12, 20, 28, 36, and 44 weeks of age, respectively)

Anterior Segment Abnormalities

Anterior segment abnormalities of DBA/2J mice included corneal calcification with or without neovascularization, progressive pigment dispersion from the iris, iris stromal atrophy, and iris transillumination defects. Iris stromal atrophy and dispersed pigment particles were visible under slit-lamp microscopy from the age of 20 weeks. From 28 weeks on, thickened pupillary borders of the iris and pupillary deformation were identifiable. All of these abnormalities became increasingly remarkable with age.

As a controversial factor associated with IOP change in DAB2J mice, corneal calcification was closely monitored in this study. At the beginning of the study, 48% (16/33) of eyes had no corneal calcification, 24% (8/33) had slight corneal calcification, and 27% (9/33) had severe corneal calcification. Before the mice were sacrificed, the corneal calcification was aggravated in three eyes, unchanged in 12 eyes, and alleviated in two eyes, compared with the baseline level. Representative images are presented in Figure 2. A total of 12 mice (24 eyes) were used to compare the histopathological changes among the three IOP groups, including 16 eyes without corneal calcification, and eight eyes with slight corneal calcification.

Light Microscopy

In DBA/2J mice with a high IOP level, iris depigmentation and ocular disorder tended to be more severe than in the mice with a normal IOP. Macroscopically, the iris of DBA/2J mice with an IOP≤10 mmHg exhibited an atypical bilayer with homogeneously heavy pigmentation (Fig. 3A). The AC angle was open. A few pigment particles were deposited in the intertrabecular spaces of the former TM (Fig. 3B). DBA/2J mice with an IOP between 10 and 15 mmHg exhibited small exudates in the AC, and their irises were thinner than those of mice with an IOP≤10 mmHg. Pigment-overloaded cells (confirmed by transmission electron microscope) were located on the anterior surface of the iris (Fig. 3C). The AC angle was narrower than that of mice with an IOP≤10 mmHg, and a large number of pigment particles were located in the TM (Fig. 3D).

Compared with the normal-IOP group, DBA/2J mice in the high-IOP group had extensive exudates in the AC. The iris stroma was reduced, and the residual iris pigment epithelial (IPE) cells were extremely stretched. The structure of the iris could no longer be identified. Pigment-overloaded cells were present in the AC and on the anterior and posterior surfaces of the iris (Fig. 3E). A large number of pigment particles were gathered in the AC angle and TM (Fig. 3F).

Transmission Electron Microscopy

Iris. Transmission electron microscopy confirmed the degeneration of the iris stroma in DBA/2J mice that was observed under light microscopy. In addition, the morphology of pigment particles between the iris stroma (round, electron-dense) and the IPE layer (oval, electron-opaque) differed noticeably at the ultrastructural level. In DBA/2J mice with an IOP≤10 mmHg, individual pigment particles were present inside the cells or surrounded by an intact membrane (Fig. 4A). In DBA/2J mice with an IOP between 10 and 15 mmHg, the number of pigment particles in the cells was more abundant than those of mice with an

Investigative Ophthalmology & Visual Science

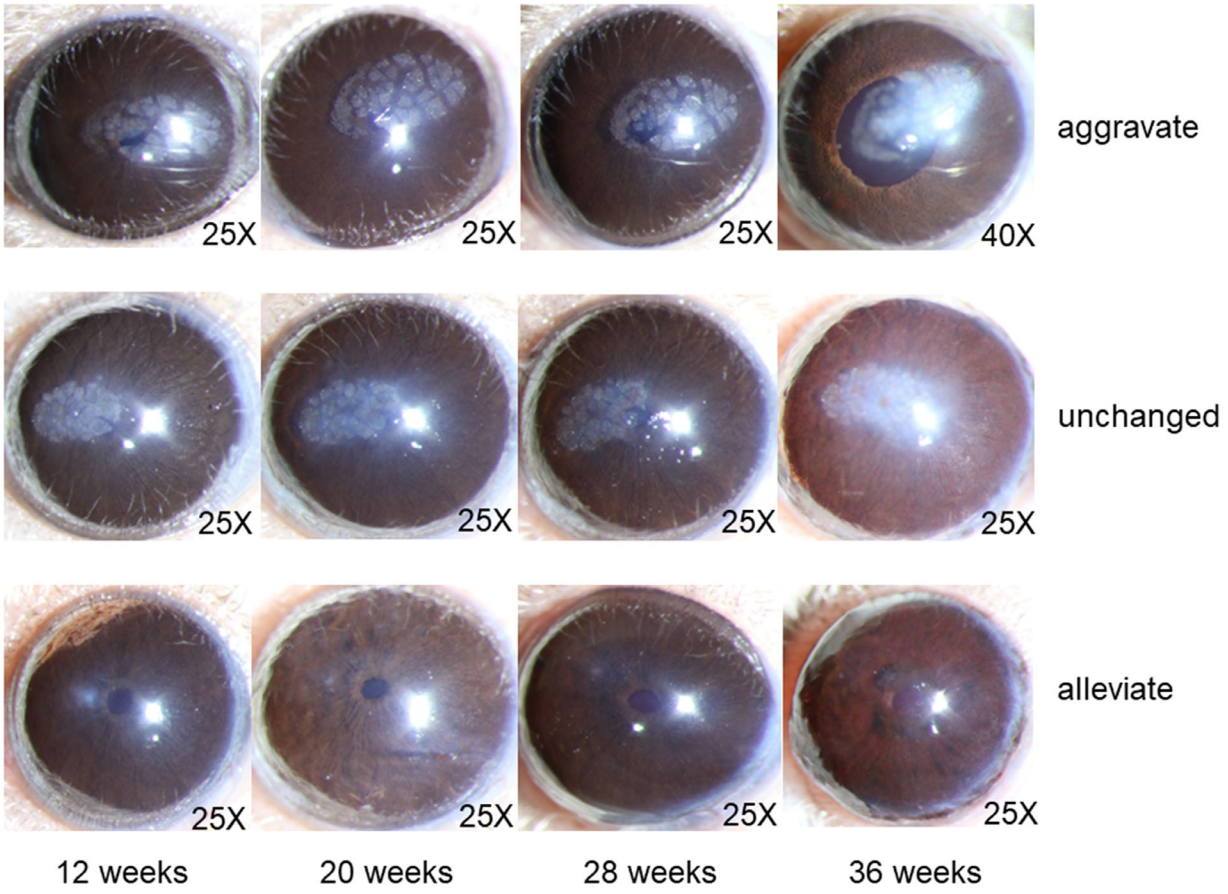

Figure 2. Representative images of the changes in corneal calcification with age in DBA/2J mice (magnification, 25× or 40×).

IOP≤10 mmHg (Fig. 4B). In DBA/2J mice with an IOP≥15 mmHg, cell debris and separate pigment particles were not observed. A large number of pigment particles were present inside the cells (Fig. 4C).

In DBA/2J mice with an IOP between 10 and 15 mmHg, pigment-overloaded cells on the anterior surface of the iris were round, had irregular boundaries, and contained a few isolated pigment particles (Fig. 5A). Small, round vacuoles were observed in these cells, probably playing a role in cell phagocytosis or the uptake of pigment particles (Fig. 5B). In DBA/2J mice with an IOP≥15 mmHg, no vacuoles were observed inside these cells, and the number of microvilli on the cellular surface increased. A large number of pigment particles were observed in these cells (Fig. 5C).

Trabecular Meshwork. In DBA/2J mice with an IOP≤10 mmHg, the intertrabecular spaces were open in some areas. Collagen fibers and elastic tissue were detected (Fig. 6A). In DBA/2J mice with an IOP between 10 and 15 mmHg, the intertrabecular spaces were narrower than in those with an IOP≤10 mmHg but not completely closed. The majority of pigment particles in the intertrabecular spaces formed clusters (Fig. 6B). In DBA/2J mice with an IOP≥15 mmHg, cell debris or separate pigment particles were extremely rare in the TM. A large number of pigment particles were present in the cells, resulting in excessive expansion of cellular volume and disappearance of intertrabecular spaces (Fig. 6C).

Separate pigment particles were occasionally detectable in the intertrabecular spaces of DBA/2J mice with an IOP between 10 and 15 mmHg (Fig. 7A). Collagen fibers and elastic tissues were drastically reduced compared to mice with a lower IOP. It is worth mentioning that isolated, free pigment particles were released from broken cells into the intertrabecular spaces (Fig. 7B). However, in DBA/2J mice with an IOP≥15 mmHg, no such particles were observed in the intertrabecular spaces.

Schlemm's Canal. In DBA/2J mice with an IOP≤10 mmHg, pigment particles were located in and around protrusions and vacuoles on the inner wall of Schlemm's canal. Only a few pigment particles were found in the lumen (Fig. 8A). DBA/2J mice with an IOP between 10 and 15 mmHg had a larger number of pigment particles around Schlemm's canal than those with a lower IOP. These pigment particles were at times so closely apposed to Schlemm's canal that it could not be determined whether they were located within the lumen (Fig. 8B).

Compared with the normal-IOP group, the high-IOP group had a smaller number of pigment particles around Schlemm's canal, with fewer protrusions and vacuoles on the inner wall. Electron-opaque clumps were observed in the lumen, which may have been red blood cells exuding from the blood vessels (Fig. 8C). However, no substantial number of pigment particles was observed in the lumen of mice with an IOP>10 mmHg. Occasionally, where the inner wall of Schlemm's canal was partially broken, a single pigment particle was observed as it was being released into the lumen of Schlemm's canal (Fig. 8D).

Investigative Ophthalmology & Visual Science

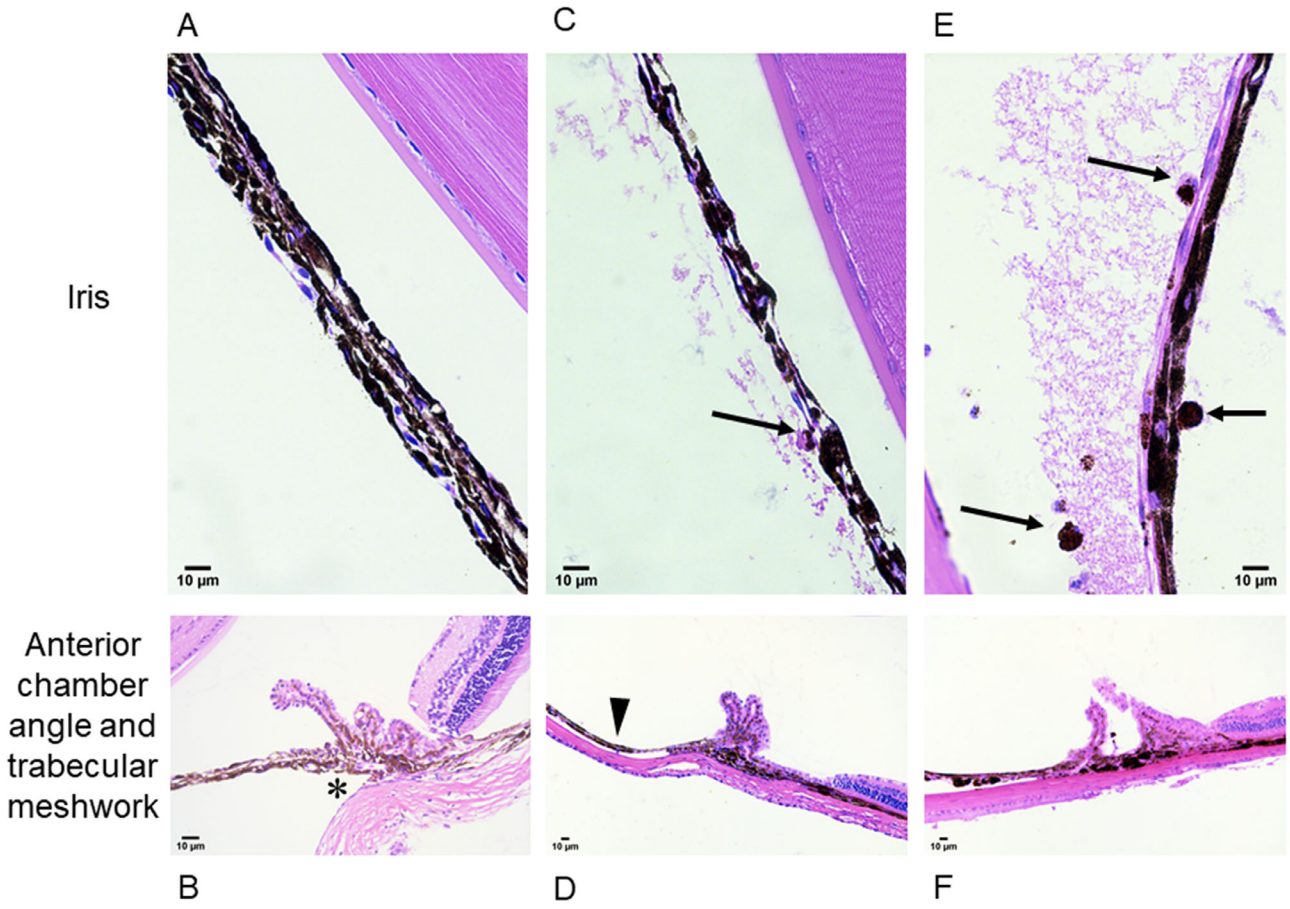

Figure 3. The iris and TM of DBA/2J mice with three different IOP levels (H&E staining). (**A**, **B**) For IOP≤10 mmHg, the atypical bilayer structure of the iris could not be readily distinguished. The AC angle was open (*asterisk*). (**C**, **D**) For 10 mmHg<IOP<15 mmHg, pigment-overloaded cells were located on the anterior surface of the iris (*large black arrow*). Peripheral anterior synechia of the iris was observed (*black arrowhead*). (**E**, **F**) For IOP≥15 mmHg, pigment-overloaded cells were distributed in the AC and on the anterior and posterior surfaces of the iris (*large black arrow*). The ciliary body and processes become short and flat. Numerous pigment particles gathered, particularly in the AC angle and TM.

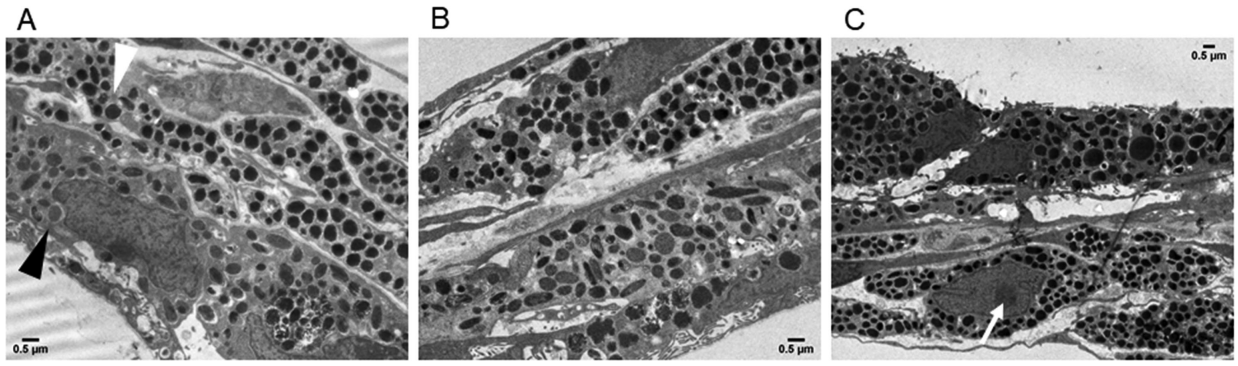

Figure 4. Ultrastructure of the iris in DBA/2J mice with three different IOP levels. (**A**) For IOP≤10 mmHg, the morphology of pigment particles differed considerably between the iris stroma (*white arrowhead*) and the IPE layer (*black arrowhead*). Iris stromal atrophy was minimal. (**B**) For 10 mmHg<IOP<15 mmHg, the degeneration of the iris stroma increased. The iris stroma was smaller, and a large number of pigment particles were present inside the cells. (**C**) For IOP≥15 mmHg, the cells were rich in pigment particles (*large white arrow*).

Investigative Ophthalmology & Visual Science

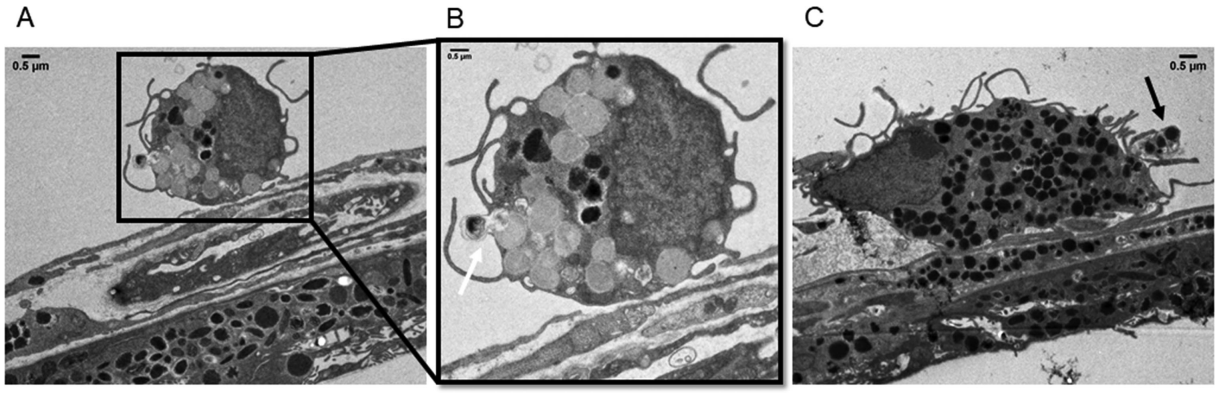

Figure 5. Ultrastructural morphology of cells on the anterior surface of the iris in DBA/2J mice with different IOP levels. (**A**, **B**) For 10 mmHg<IOP<15 mmHg, small, round cells with irregular boundaries were located on the anterior surface. Small, round vacuoles were observed in these cells. The microvilli on the cellular surfaces were probably assisting the cells in their uptake of pigment particles (*large white arrow*). (**C**) For IOP≥15 mmHg, extracellular pigment particles were discovered (*large black arrow*). Large numbers of pigment particles were also present in the cells. The cellular nuclei were compressed to one side.

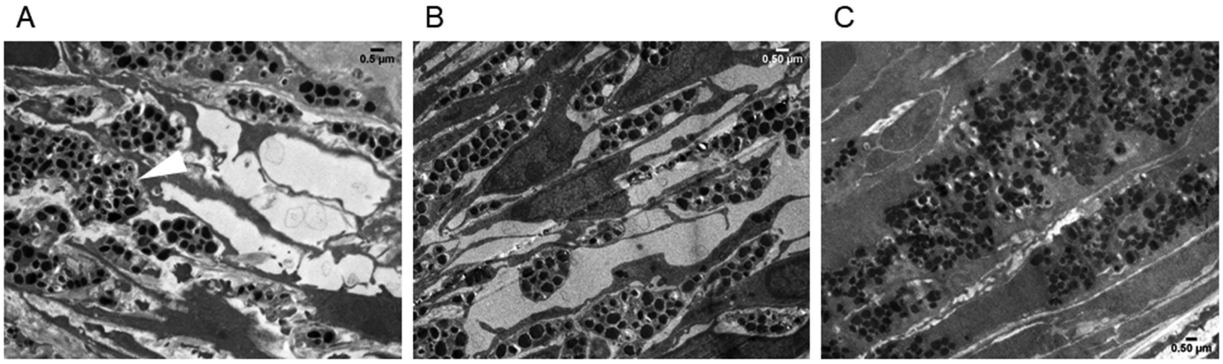

Figure 6. Ultrastructure of the TM in DBA/2J mice with different IOP levels. (**A**) For IOP≤10 mmHg, a few pigment particles were surrounded by an intact membrane in the intertrabecular spaces (*white arrowhead*). (**B**) For 10 mmHg<IOP<15 mmHg, the intertrabecular spaces were narrower but remained open in certain areas. (**C**) For IOP≥15 mmHg, numerous individual pigment particles were found in the cells. Cell debris and separate pigment particles were extremely rare in the TM. No intertrabecular spaces were observed.

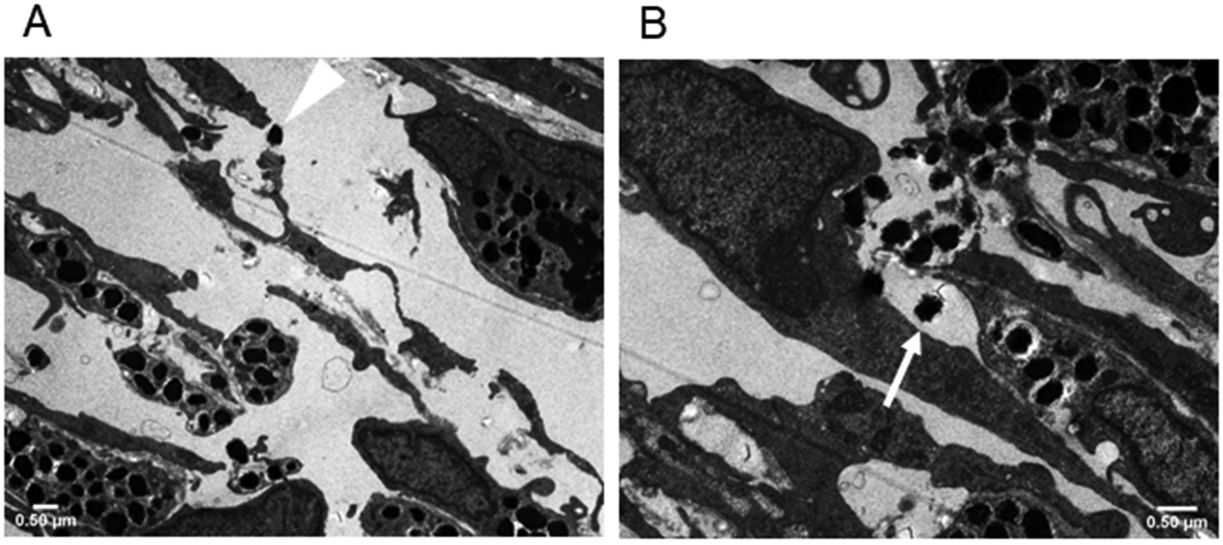

Figure 7. Ultrastructure of the TM in DBA/2J mice with an IOP at a critical level (10–15 mmHg). (**A**) Separate pigment particles (*white arrowhead*) were occasionally visible in the intertrabecular spaces. (**B**) Separate pigment particles (*large white arrow*) were released from broken cells into the intertrabecular spaces.

Investigative Ophthalmology & Visual Science

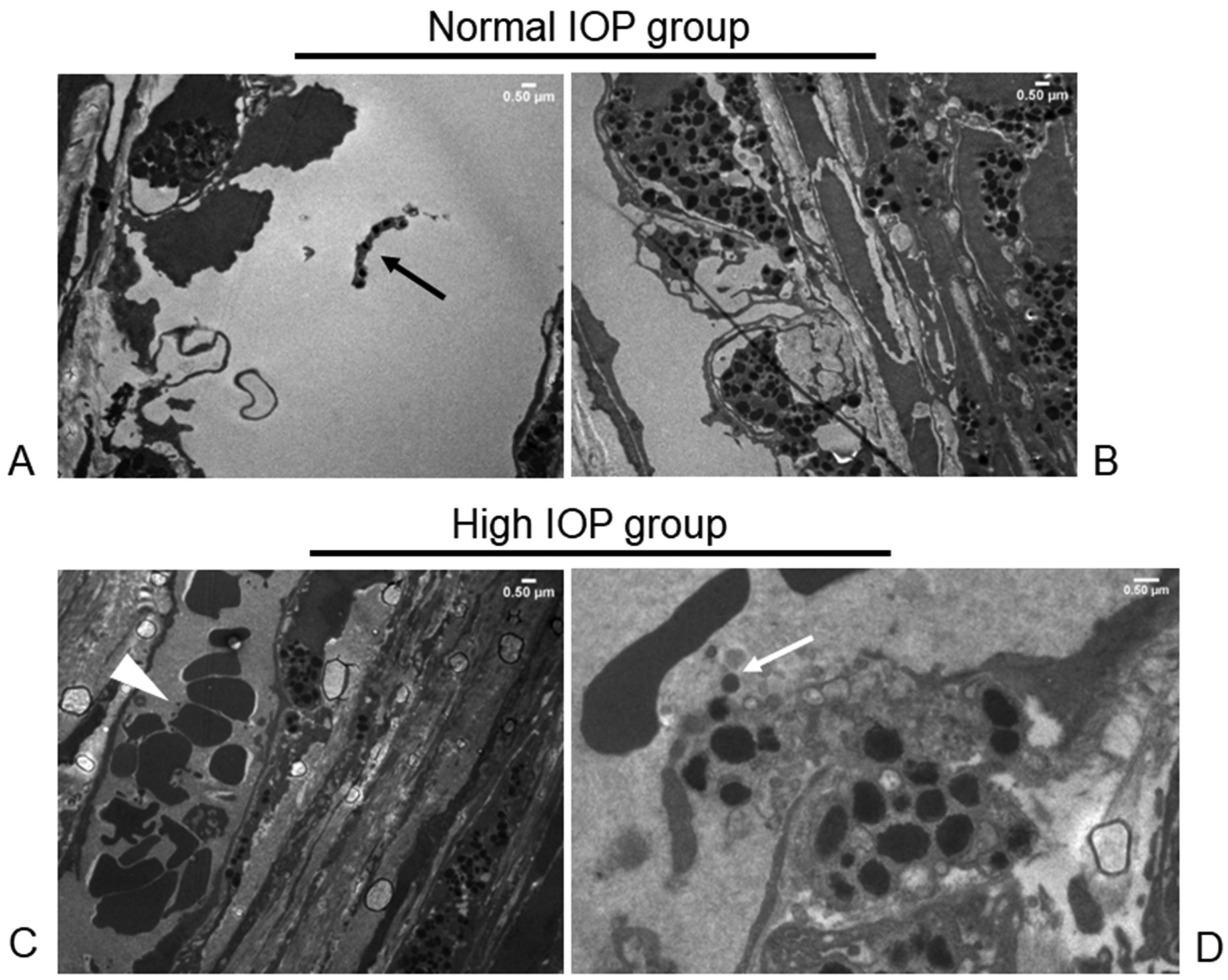

Figure 8. Ultrastructure of Schlemm's canal in DBA/2J mice with different IOP levels. (**A**) For IOP≤10 mmHg, pigment particles were located around Schlemm's canal. Only a few pigment particles were present in the lumen (*large black arrow*). (**B**) For 10 mmHg<IOP<15 mmHg, pigment particles around Schlemm's canal were more abundant than for those with an IOP≤10 mmHg. (**C**) For IOP≥15 mmHg, the lumen of Schlemm's canal was filled with electron-opaque clumps (*white arrowhead*), and a small number of pigment particles were distributed around Schlemm's canal. (**D**) Also for IOP≥15 mmHg, isolated, free pigment particles were released into the lumen of Schlemm's canal after the rupture of the inner wall basement membrane (*large white arrow*).

Diameters of Pigment Particles and Their Relationship with IOP

Anterior Chamber. The majority of pigment particles in the AC were small and round (187/252, 74.2%), with an average diameter of 0.38±0.09 μm (range, 0.20–0.73). The minority of particles were big and oval (65/252, 25.8%), with an average length of 0.69±0.17 μm (range, 0.35–1.20). These pigment particles were sorted from smallest to largest and grouped by 25th (0.4 μm) and 75th (0.8 μm) percentiles. We divided the particles into three different sizes: large (≥0.8 μm), medium (>0.4 μm and <0.8 μm), and small (≤0.4 μm). With 100 random selections, 37% (28/75) of round pigment particles had a diameter >0.4 μm and 96% (24/25) of oval pigment particles had a length of >0.4 μm (Fig. 9).

Iris. In DBA/2J mice with an IOP≤10 mmHg, 68.3% (286/419) of pigment particles were round, with an average diameter of 0.55±0.10 μm (range, 0.25–0.79); oval particles accounted for 31.7% (133/419), with an average length of 0.85±0.12 μm (range, 0.63–1.16). In DBA/2J mice with an IOP between 10 and 15 mmHg, 68.8% (141/205) of pigment particles were round, with an average diameter of 0.54±0.15 μm (range, 0.29–1.14); oval particles accounted for 31.2% (64/205), with an average length of 0.85±0.15 μm (range, 0.57–1.15). In DBA/2J mice with an IOP≥15 mmHg, 56.4% (239/424) of pigment particles were round, with an average diameter of 0.56±0.12 μm (range, 0.29–0.81); oval particles accounted for 43.6% (185/424), with an average length of 0.81±0.15 μm (range, 0.56–1.27).

With 100 random selections, the proportion of round pigment particles with a diameter >0.40 μm in DBA/2J mice with the three different IOP levels (from normal to high) were 96% (65/68), 86% (59/69), and 93% (52/56), respectively. In contrast, all oval pigment particles had a length >0.40 μm (32/32, 31/31, and 44/44, respectively). There was no statistically significant difference in the diameters of round pigment particles (F=0.962, P=0.386) or the lengths of oval pigment particles (F=0.157, P=0.854) among the three IOP groups (Figs. 10A, 10B).

Trabecular Meshwork. In DBA/2J mice with an IOP≤10 mmHg, 52.4% (87/166) of pigment particles were round, with an average diameter of 0.44±0.13 μm (range, 0.19–0.75); oval particles accounted for 47.6% (79/166), with an average length of 0.65±0.14 μm (range, 0.43–0.95).

Investigative Ophthalmology & Visual Science

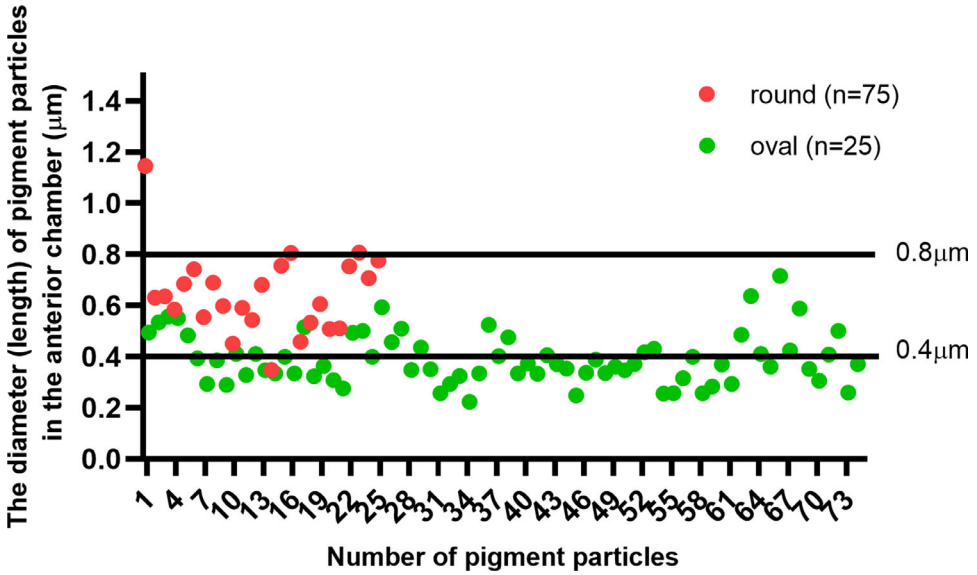

Figure 9. Distribution of pigment particles in the AC of DBA/2J mice. The *red dots* represent the diameters of the round pigment particles (n=75); the *green dots* represent the length of the oval pigment particles (n=25). The *bottom* and *top thick lines* indicate the 25th (0.4 μm) and 75th (0.8 μm) percentiles, respectively.

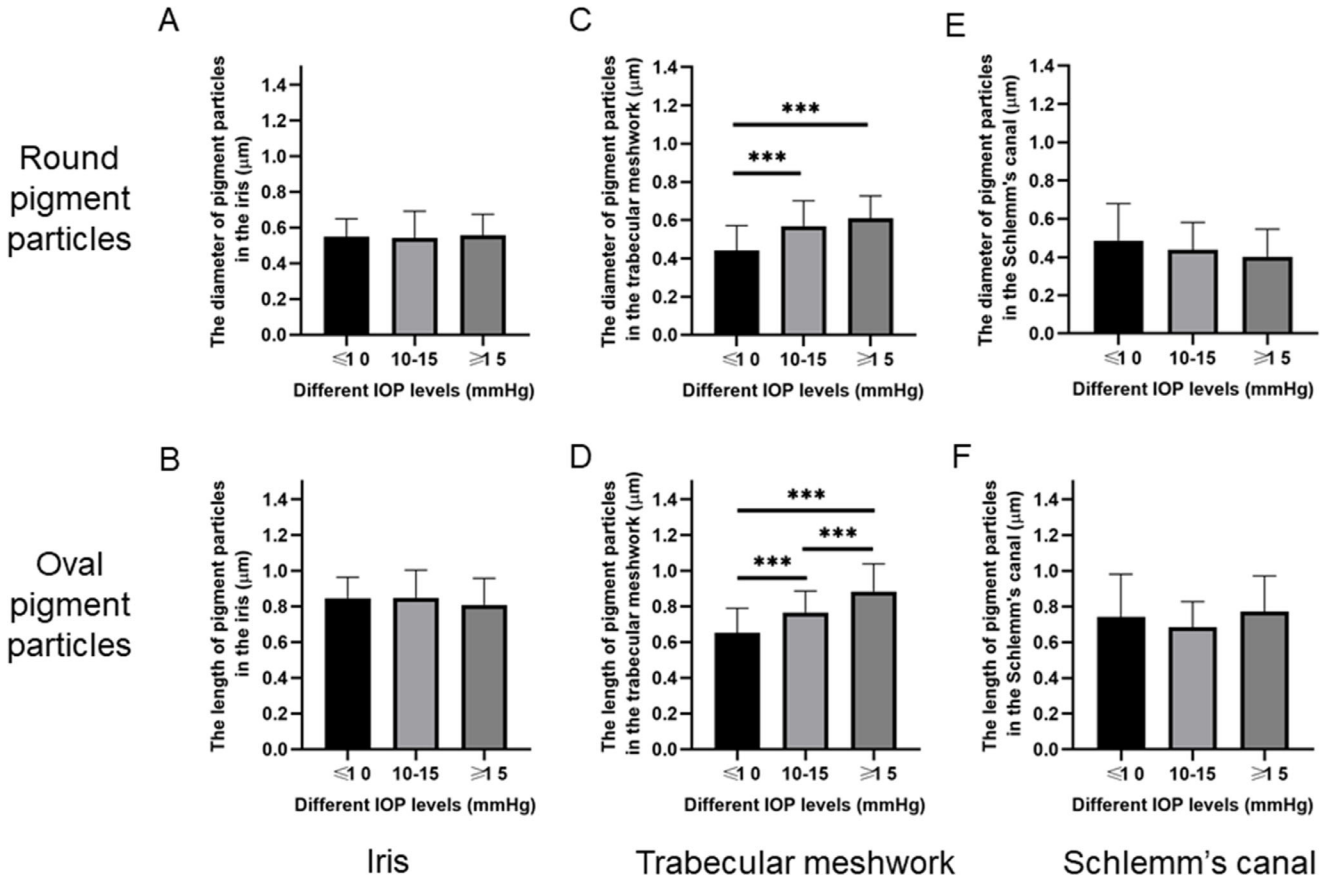

Figure 10. Distribution of pigment particles in the iris, TM, and around Schlemm's canal in DBA/2J mice with three IOP levels. *Error bars* represent the standard error of the mean. (**A**, **B**) In the iris, there were no statistically significant differences in the diameters of round particles or the lengths of oval particles among the three IOP groups. (**C**, **D**) In the TM, the diameters of round pigment particles (IOP≤10 mmHg, 0.44±0.13 μm; IOP between 10 and 15 mmHg, 0.57±0.13 μm; IOP≥15 mmHg, 0.61±0.12 μm) and the lengths of oval pigment particles (0.65±0.14 μm, 0.77±0.12 μm, and 0.88±0.15 μm, respectively) among the three IOP groups were statistically significantly different. $^{***}P<0.001$. (**E**, **F**) Around Schlemm's canal, no statistically significant differences were present.

Investigative Ophthalmology & Visual Science

In DBA/2J mice with an IOP between 10 and 15 mmHg, 61.4% (137/223) of pigment particles were round, with an average diameter of 0.57±0.13 µm (range, 0.31–0.83); oval particles accounted for 38.6% (86/223), with an average length of 0.77±0.12 µm (range, 0.55–1.10). In DBA/2J mice with an IOP≥15 mmHg, 68.9% (284/412) of pigment particles were round, with an average diameter of 0.61±0.12 µm (range, 0.43–0.91); oval particles accounted for 31.1% (128/412), with an average length of 0.88±0.15 µm (range, 0.62–1.18).

For each IOP group (from normal to high), among 100 randomly selected pigment particles, the proportions of round pigment particles with a diameter >0.40 µm in the three IOP levels were 56% (29/52), 92% (56/61), and 100% (69/69), respectively. In contrast, all oval pigment particles had a length >0.40 µm (48/48, 39/39, and 31/31, respectively). The differences in the diameters of round pigment particles (F=27.258, P<0.001) and the lengths of oval pigment particles (F=27.295, P<0.001) in the TM among the three IOP groups were statistically significantly different (Figs. 10C, 10D).

Schlemm's Canal. In DBA/2J mice with an IOP≤10 mmHg, 65% (11/17) of pigment particles were round, with an average diameter of 0.49±0.19 µm (range, 0.26–0.84); oval particles accounted for 35% (6/17), with an average length of 0.74±0.24 µm (range, 0.44–1.06). Counting all particles in the field of view around Schlemm's canal, the diameters of 55% (6/11) of the round particles and the lengths of all six oval particles were >0.4 µm. In this IOP group, the diameter of all three round pigment particles (range, 0.41–0.47 µm) and the lengths of oval particles (range, 0.47–0.49 µm) within Schlemm's canal were >0.4 µm.

In DBA/2J mice with an IOP between 10 and 15 mmHg, 58% (76/130) of pigment particles were round, with an average diameter of 0.44±0.14 µm (range, 0.22–0.76); oval particles accounted for 42% (54/130), with an average length of 0.68±0.14 µm (range, 0.45–1.11). Among 100 randomly selected pigment particles, the diameters of 50% (29/58) of the round particles and the lengths of all 42 of the oval particles were >0.4 µm.

In DBA/2J mice with an IOP≥15 mmHg, 46% (11/24) of pigment particles were round, with an average diameter of 0.40±0.14 µm (range, 0.25–0.71); oval particles accounted for 54% (13/24), with an average length of 0.77±0.20 µm (range, 0.44–1.07). Counting all pigment particles in the field of view, the diameters of 27% (3/11) of the round particles and the lengths of all 13 of the oval particles were >0.4 µm. No pigment particles were observed in Schlemm's canal in the latter two IOP groups.

Comparison of the pigment particles around Schlemm's canal in DBA/2J mice of different IOP groups revealed that the differences in the diameters of round pigment particles (F=1.476, P=0.237) and the lengths of oval pigment particles (F=0.852, P=0.431) were not statistically significant (Figs. 10E, 10F).

Discussion

In this study, we observed a great diversity in the distribution of pigment particles in the aqueous drainage structures of DBA/2J mice with different IOP levels. We confirmed the presence of an MPD for pigment particles in the TM of DBA/2J mice by using transmission electron microscopy combined with ImageJ-based analysis. Pigment particles with diameters≤MPD could pass freely through the aqueous drainage structures, whereas pigment particles with diameters >MPD were restricted in the TM of DBA/2J mice.

The development of PG in DBA/2J mice appears to be complex. Herein, DBA/2J mice at different ages were divided into three groups depending on the level of the IOP before they were sacrificed: (1) ≤10 mmHg; (2) between 10 and 15 mmHg; and (3) ≥15 mmHg. In DBA/2J mice with an IOP≤10 mmHg, pigment particles in the intertrabecular spaces were located inside the cells or surrounded by an intact membrane, but cell debris and separate pigment particles were relatively rare. Similar results were described in another study.[10] In DBA/2J mice with an IOP between 10 and 15 mmHg, pigment-overloaded cells were deposited on the anterior surface of the iris, likely playing an important role in phagocytic uptake of pigment. To our knowledge, this has not been discussed in previous studies. In DBA/2J mice with an IOP≥15 mmHg, pigment-overloaded cells were widely present in the AC and on the anterior and posterior surfaces of the iris. Such cells were previously identified as macrophages, exclusively located on the anterior surface of the iris in 9-month-old DBA/2J mice.[10] These discrepancies may be due to the varying onset time and degree of IOP elevation among DBA/2J mice of different ages.[7,9] Grouping by age alone has certain limitations.

The pigment particles in the iris differed considerably in morphology and quantity. In general, round pigment particles were predominant in the iris stroma, whereas the IPE layer contained a majority of oval pigment particles. However, the sizes of the pigment particles did not differ among the three IOP groups (P>0.05). When iris stromal degeneration began, pigment particles detached from the iris and entered the AC. We classified these particles into three groups based on size: large (≥0.8 µm), medium (>0.4 µm and <0.8 µm), and small (≤0.4 µm). The majority of pigment particles observed in the AC of DBA/2J mice were medium or large. Subsequently, pigment particles of various sizes were transferred to the TM via the aqueous convection current. In the high-IOP group (IOP≥15 mmHg), a larger number of pigment particles were restricted to the TM than in mice with a lower IOP, and the sizes were larger (P<0.001). In these mice, all individual pigment particles were >0.4 µm in size. Likewise, although the number of pigment particles restricted to the TM was lower in the normal-IOP group, the majority were also >0.4 µm in size. Our results indicate that the IOP elevation in DBA/2J mice was closely related to the deposition of large and medium pigment particles in the TM.

Remarkably, we found that cells in the TM had ruptured and released free pigment particles into the intertrabecular space in DBA/2J mice with an IOP between 10 and 15 mmHg. However, no isolated, extracellular pigment particles were observed in DBA/2J mice with an IOP≥15 mmHg. Free-floating pigment particles only exist in the intertrabecular space for a short period of time, after which they may be transferred downstream of the aqueous drainage channels or taken up by other cells in the TM. These results suggest that certain temporary structural changes may have previously been overlooked in DBA/2J mice with an IOP at a critical level (between 10 and 15 mmHg). Furthermore, in that case, large and medium particles in the TM comprised 92% of all particles, but the total number of particles was not enough to significantly increase the aqueous outflow resistance. Hence, the IOP can still be compensated to within the normal range.

Investigative Ophthalmology & Visual Science

For DBA/2J mice, 0.4 µm may be an MPD, as small pigment particles seem to be very rare in the TM of those with high IOP levels. There may be a similar MPD in human aqueous drainage structures, although we are aware of no such finding being described to date. DBA/2J mice develop ocular abnormalities like those observed in patients with pigment dispersion syndrome (PDS) and PG. However, the size of pigment particles in DBA/2J mice was different from those previously described in humans; the latter were slightly larger in diameter.[4] Thus, although DBA/2J mice have a pathogenesis of PDS/PG similar to that of humans, data obtained from this mouse strain may not be comparable to that from humans.

In DBA/2J mice, it has long been thought that the degree of TM pigmentation is highly associated with increased outflow resistance. John et al.[8] reported that DBA/2J mice developed a form of secondary angle-closure glaucoma and that these manifestations became increasingly severe with age. Similarly, Scholz et al.[9] found that DBA/2J mice had a narrowed chamber angle due to an anteriorly displaced ciliary body, which also obstructed the aqueous humor outflow. In our study, two phenomena were observed in these mice. First, under natural conditions, the IOP of DBA/2J mice increased gradually from 12 to 36 weeks but showed a downward trend from then on. Second, light and transmission electron microscopy revealed that the anterior synechia associated with angle closure became increasingly severe with age (data not shown). If angle closure is the major contributor to IOP elevation in DBA/2J mice, it would be difficult to explain why the IOP decreases from 36 weeks on but angle closure becomes increasingly severe.

This study had several limitations. First, some characteristics of angle closure may be involved in IOP elevation in DBA/2J mice. Such findings have also been reported in previous studies.[8,9] However, it is technically difficult so far to distinguish the two components—pigment particle obstruction and angle closure—in the mechanism of IOP elevation in DBA/2J mice. To minimize the interference from angle closure, the relationship between the distribution of pigment particles and IOP elevation was established at an early stage of the animal model, during which angle closure usually has not come into being. Second, it was difficult for us to compare the sizes of pigment particles in the AC of DBA/2J mice among groups with different IOP levels due to limitations in the technology. We compared the sizes of pigment particles in the iris of DBA/2J mice, which was thought to be an indirect method to determine whether pigment granules in the AC differ among groups. Finally, a substantial number of intracellular particles were present in the TM of DBA/2J mice, resulting in expansion of cellular volume and disappearance of intertrabecular spaces. This differs from the ultrastructure of the TM described in patients with PG.[1,2,4,11,12] Further study is necessary to determine how these pigment particles enter the cells in DBA/2J mice.

In summary, we provide evidence of an MPD in the aqueous drainage structures of DBA/2J mice. Pigment particles with diameters >0.4 µm may lead to aqueous outflow obstruction and IOP elevation. In contrast, smaller pigment particles may play a limited role in the pathogenesis of glaucoma. Theoretically, if one could convert large and medium pigment particles into small ones at an early stage, it would assist in the prevention and treatment of PDS/PG. Such findings may provide a new therapeutic approach in the future.

Acknowledgments

Supported by grants from the National Natural Science Foundation of China (81170845 and 81970795).

Disclosure: **L. Pu**, None; **R. Zhou**, None; **Q. Li**, None; **G. Qing**, None

References

1. Murphy CG, Johnson M, Alvarado JA. Juxtacanalicular tissue in pigmentary and primary open angle glaucoma. The hydrodynamic role of pigment and other constituents. *Arch Ophthalmol.* 1992;110(12):1779–1785.
2. Alvarado JA, Murphy CG. Outflow obstruction in pigmentary and primary open angle glaucoma. *Arch Ophthalmol.* 1992;110(12):1769–1778.
3. Richardson TM, Hutchinson BT, Grant WM. The outflow tract in pigmentary glaucoma: a light and electron microscopic study. *Arch Ophthalmol.* 1977;95(6):1015–1025.
4. Shimizu T, Hara K, Futa R. Fine structure of trabecular meshwork and iris in pigmentary glaucoma. *Albrecht von Graefes Arch Klin Exp Ophthalmol.* 1981;215(3):171–180.
5. Anderson MG, Smith RS, Hawes NL, et al. Mutations in genes encoding melanosomal proteins cause pigmentary glaucoma in DBA/2J mice. *Nat Genet.* 2002;30(1):81–85.
6. Libby RT, Anderson MG, Pang IH, et al. Inherited glaucoma in DBA/2J mice: pertinent disease features for studying the neurodegeneration. *Vis Neurosci.* 2005;22(5):637–648.
7. Turner AJ, Vander Wall R, Gupta V, Klistorner A, Graham SL. DBA/2J mouse model for experimental glaucoma: pitfalls and problems. *Clin Exp Ophthalmol.* 2017;45(9):911–922.
8. John SW, Smith RS, Savinova OV, et al. Essential iris atrophy, pigment dispersion, and glaucoma in DBA/2J mice. *Invest Ophthalmol Vis Sci.* 1998;39(6):951–962.
9. Scholz M, Buder T, Seeber S, Adamek E, Becker CM, Lütjen-Drecoll E. Dependency of intraocular pressure elevation and glaucomatous changes in DBA/2J and DBA/2J-Rj mice. *Invest Ophthalmol Vis Sci.* 2008;49(2):613–621.
10. Schraermeyer M, Schnichels S, Julien S, Heiduschka P, Bartz-Schmidt KU, Schraermeyer U. Ultrastructural analysis of the pigment dispersion syndrome in DBA/2J mice. *Graefes Arch Clin Exp Ophthalmol.* 2009;247(11):1493–1504.
11. Tektas OY, Lütjen-Drecoll E. Structural changes of the trabecular meshwork in different kinds of glaucoma. *Exp Eye Res.* 2009;88(4):769–775.
12. Buffault J, Labbé A, Hamard P, Brignole-Baudouin F, Baudouin C. The trabecular meshwork: structure, function and clinical implications. A review of the literature. *J Fr Ophtalmol.* 2020;43(7):e217–e230.
13. Zeiss CJ, Tu DC, Phan I, Wong R, Treuting PM. Special senses: eye. In: Treuting PM, Dintzis SM, Montine KS , eds. *Comparative Anatomy and Histology: A Mouse, Rat, and Human Atlas*. 2nd ed. London: Academic Press; 2018:445–470.
14. Tsuchiya S, Higashide T, Hatake S, Sugiyama K. Effect of inhalation anesthesia with isoflurane on circadian rhythm of murine intraocular pressure. *Exp Eye Res.* 2021;203:108420.
15. Wang WH, Millar JC, Pang IH, Wax MB, Clark AF. Noninvasive measurement of rodent intraocular pressure with a rebound tonometer. *Invest Ophthalmol Vis Sci.* 2005;46(12):4617–4621.
16. Epstein DL, Freddo TF, Anderson PJ, Patterson MM, Bassett-Chu S. Experimental obstruction to aqueous outflow by pigment particlesin living monkeys. *Invest Ophthalmol Vis Sci.* 1986;27(3):387–395.
17. Dang Y, Waxman S, Wang C, Loewen RT, Sun M, Loewen NA. A porcine ex vivo model of pigmentary glaucoma. *Sci Rep.* 2018;8(1):5468.